Charge-Transfer Complex Crystal Based on Extended-π-Conjugated Acceptor and Sulfur-Bridged Annulene: Charge-Transfer Interaction and Remarkable High Ambipolar Transport Characteristics

Yunke Qin, Jing Zhang, Xiaoyan Zheng, Hua Geng, Guangyao Zhao, Wei Xu,* Wenping Hu, Zhigang Shuai,* and Daoben Zhu*

Organic donor–acceptor complexes, which consist of electron donor and acceptor molecules with typical mixed or segregated stack motif, generally display unique crystalline structure and optoelectronic properties. Since the discovery of the donor–acceptor charge-transfer (CT) crystal tetrathiafulvalene-tetracyanoquinodimethane (TTF–TCNQ), molecular donor–acceptor complexes have been paid increasing attention in organic electronics.[1] Apart from the individual properties of the donor or acceptor in the complex, promising features that originate from the combination and/or intermolecular interactions have been theoretically and experimentally confirmed such as electrical conductivity,[2] ferroelectricity,[3] photovoltaic effects,[4] and optical properties.[5] Ambipolar transport behavior in such donor–acceptor (D–A) complexes was first reported by T. Hasegawa et al. with (BEDT–TTF)(F$_2$TCNQ) at low temperature in 2004.[6] After that, other two TTF-derivative-based donor–acceptor complexes were reported to be ambipolar materials, DBTTF–TCNQ[7] (DBTTF = dibenzothiatetrathiafulvalene) and (BEDT–TTF)(TCNQ) (BEDT-TTF = bis(ethylenedithio)tetrathiafulvalene).[8] A recent theoretical calculation on three typical mixed-stack charge-transfer complexes, including DBTTF–TCNQ, revealed that such materials could possess extremely high hole and electron mobilities simultaneously, as there are strong electronic couplings along the alternative stacking direction due to the superexchange mechanism.[9] Besides TTF-based materials, we found a novel donor molecule meso-diphenyl tetrathia[22]annulene[2,1,2,1] (DPTTA)

could form D–A complexes with tetracyanoquinodimethane (TCNQ)[10] and fullerenes[11] through a solution procedure. All these co-crystals displayed efficient ambipolar transport properties. In the former case, DPTTA and TCNQ stack alternatively into columns to form ribbon-shaped microcrystals, which display air-stable and balanced ambipolar transport properties with electron and hole mobilities up to 0.03 and 0.0 cm^2 V^{-1} s^{-1}. Such behavior is rationalized by quantum calculations on superexchange effects in the intermolecular electronic couplings and molecular reorganization energy. In the latter cases, DPTTA and fullerenes (C60, C70) formed 2D segregated alternating layer structures, where continuing π–π interactions existed both in donor and acceptor layers, which serve as transport paths for holes and electrons, separately. These experimental and theoretical works revealed that D–A complexes with either mixed- or segregated-stack structures could be ambipolar semiconductors, and have stimulated continuous efforts in developing ambipolar materials with this combinational approach besides chemical tailoring strategies. Recently, more D–A co-crystals with ambipolar behavior were realized. Wakahara et al. reported a ambipolar transistor based on C$_{60}$-cobalt porphyrin (1:1) co-crystal which displayed a balance of electron and hole mobilities in the range of 10^{-5}–10^{-6} cm^2 V^{-1} s^{-1}.[12] Park et al. developed a isometric donor–acceptor co-crystal with donor and acceptor molecules both based on distyrylbenzene, which displayed strong red emission property as well as p-/n-type field-effect mobility up to 6.7 × 10^{-3} and 6.7 × 10^{-2} cm^2 V^{-1} s^{-1}.[13] A reinvestigation of solution-processed DBTTF–TCNQ crystals revealed hole and electron mobilities of 0.04 and 0.13 cm^2 V^{-1} s^{-1}, respectively.[14] Despite these recent experimental and theoretical achievements, D–A complexes with stable ambipolar transport properties in ambient atmosphere still meet with limited success. The donor or acceptor molecules employed are still limited to TCNQ, TTF, acenes, and fullerenes and their derivatives. No donor–acceptor co-crystals with electron and hole mobility both exceeding 0.1 cm^2 V^{-1} s^{-1} were reported yet. Improving the carrier mobility through this combination approach remains a tough challenge. More experimental and theoretical research is demanded.

Herein, we present the first example of D–A complexes with both electron and hole field-effect mobilities exceeding 0.1 cm^2 V^{-1} s^{-1}. A TCNQ derivative, 4,8-bis(dicyanomethylene)-4,8-dihydrobenzo[1,2-b:4,5-b′]-dithiophene (DTTCNQ) with extended π-conjugated system was employed instead of TCNQ

Y. Qin, J. Zhang, X. Zheng, Dr. H. Geng, G. Zhao,
Prof. W. Xu, Prof. W. Hu, Prof. Z. Shuai, Prof. D. Zhu
Beijing National Laboratory for Molecular Sciences
Key Laboratory of Organic Solids
Institute of Chemistry
Chinese Academy of Sciences
Beijing 100190, P. R. China
E-mail: wxu@iccas.ac.cn; zgshuai@tsinghua.edu.cn
zhudb@iccas.ac.cn
X. Zheng, Prof. Z. Shuai
Chemistry Department
Tsinghua University
Beijing 100084, P. R. China
Y. Qin, J. Zhang, G. Zhao
University of Chinese Academy of Sciences
Beijing 100049, P. R. China

COMMUNICATION
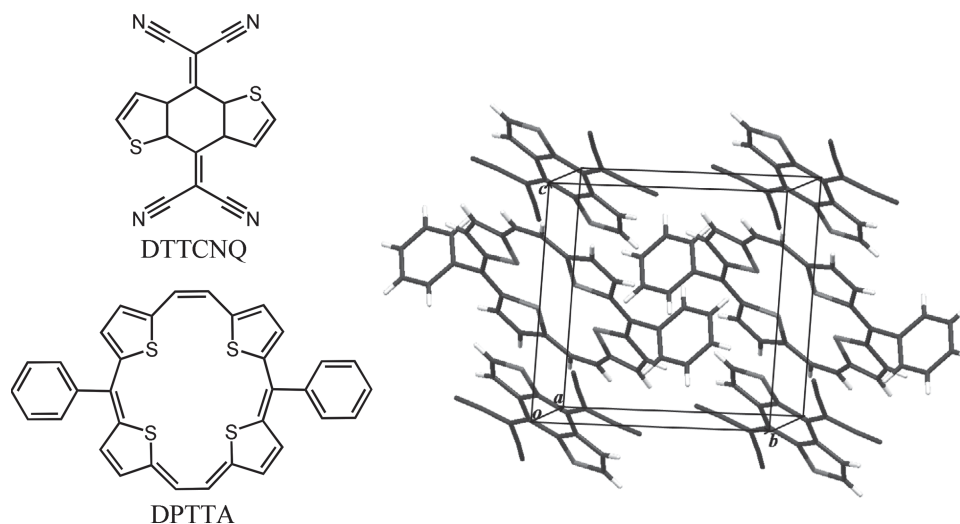
Scheme 1. Chemical structure of DPTTA and DTTCNQ and the extended packed unit cell of the resulted co-crystal in capped stick representation. The disordered orientation of DTTCNQ is omitted for clarity.

to form a complex with DPTTA in 1:1 ratio (**Scheme 1**) with the rationalization that the intermolecular electronic couplings among D–A molecules should be enhanced by employing such an acceptor molecule with a π-conjugated system that better matches that of the donor molecule, which may facilitate the superexchange effect and enhance the charge-transport properties. Crystal-structure analysis and quantum calculations rationalized the ambipolar transport properties and revealed the existence of both direct coupling and superexchange interactions which resulted in a quasi-2D transport network.

DPTTA was selected as the model donor owing to its electron-rich aromatic macrocyclic structure, moderate hole-transport property,[15] and excellent assembly ability with acceptors.[10,11] Further exploration of the DPTTA-based donor–acceptor system is necessary. TCNQ is a classical organic electron acceptor that has played an important role in the field of organic electronics. TCNQ's conjugation and electron-accepting ability can be adjusted by introducing substituents or by annulations (extension of the π-system). DTTCNQ, a thiophene-fused TCNQ-type acceptor, can form highly conducting charge-transfer complex with TTF and a conducting salt with tetraethylammonium.[16] The first half-wave reductive potential ($E_{red1}^{1/2}$) of DTTCNQ is 0.13 V vs. SCE,[16a] which is more negative than that of TCNQ (about 0.17 V vs. SCE),[16b] which indicates a weaker electron-accepting ability. The LUMO energy of this acceptor can be estimated as −4.53 eV by using the formula LUMO = −4.4 eV − $E_{red1}^{1/2}$.[17] An increase of the conjugated system is thought to be of great importance in enhancing the π–π stacking.

For TCNQ-type acceptors, the CN frequency shift in the infrared absorption spectrum (IR) has been widely used for detecting the charge-transfer ratio.[18] In this DPTTA–DTTCNQ complex, a 5 cm^{-1} frequency shift of the signal arising from CN can be observed that indicates a small degree of charge transfer between the donor and acceptor (Figure S1). No significant shifting of maximum absorption or CT absorption band is detected in the ground state from the UV-vis absorption spectrum in a dilute solution of chlorobenzene (Figure S2),

probably due to the weak charge-transfer interaction at low concentrations. To further verify the charge-transfer property of the DPTTA–DTTCNQ complex, an electron spin resonance spectrum (ESR), an effective method in identification of active radicals, was recorded. The spectrum also confirms the existence of D–A charge-transfer interactions (Figure S3). A strong resonance signal occurred centered at 348 mT with a line-width of several milliTesla. According to ESR theory, the g factor is given by Equation (1):

$$h\gamma = g\mu_{B}H_{center} \tag{1}$$

where h, γ, μ_B, and H_{center} are the Planck constant, frequency of the applied microwave magnetic field, Bohr magnetron, and resonance magnetic field, respectively. Thus, the g factor can be easily determined: $g = 2.0068$, which nearly equals to the free-electron value of 2.0023, and which illustrates the existence of unpaired electrons in the complex.

Diffuse reflectance spectroscopy (DRS) was also carried out (Figure S4A). Compared with the spectra of DPTTA and DTTCNQ, there is a new distinct broad band between 800–2500 nm in the spectrum of the DPTTA–DTTCNQ complex; this is an indication of some degree of electron interaction between DPTTA and DTTCNQ. The new broad band can be assigned as the charge-transfer absorption band and may be associated with the transition from the ground state of the complex to the first excited state.[19] For semiconductor materials, DRS is also used to study the energy band structure. The bandgap can be estimated by the Kubelka–Munk function[20] as follows in Equation (2):

$$h(\nu\alpha)^{1/n} = h\nu - Eg \tag{2}$$

where α is the absorption coefficient, ν is frequency of vibration, and Eg is the bandgap. The value of the exponent n is determined by the nature of the transition, that is, for direct allowed transitions $n = 1/2$ and for indirect allowed transitions $n = 2$. The involvement of the phonon makes the indirect
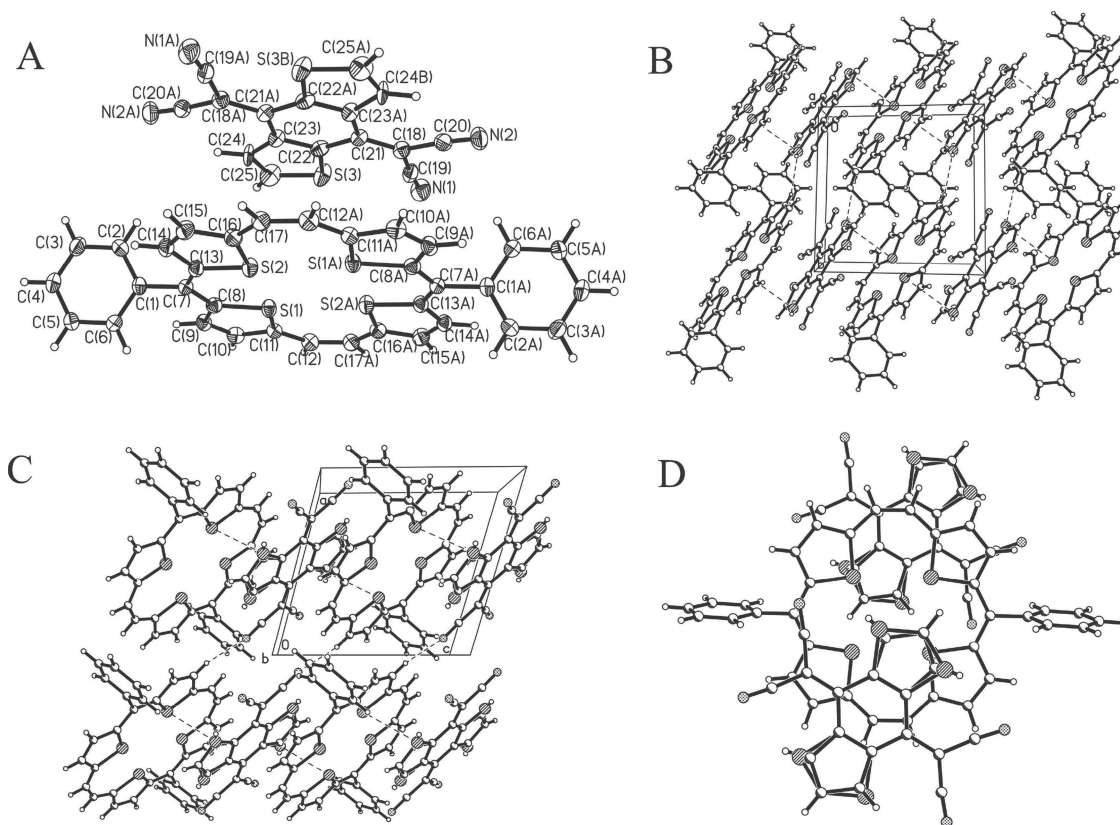
Figure 1. Crystal structure of DPTTA–DTTCNQ co-crystal. A) Molecular structure of DPTTA–DTTCNQ with 50 % probability ellipsoids (the disordered orientation of DTTCNQ are omitted for clarity). B) Crystal packing view along *a* axis. C) Stacking pattern view along *b* axis (the dashed line indicates the nonbonding interactions). D) Overlap pattern between DPTTA and DTTCNQ (view perpendicular to the DPTTA plane).

process much less likely to occur, so $n = 1/2$ is used for our complex sample. The $(h\nu\alpha)^2$–$h\nu$ curve was drawn and the optical bandgap was estimated to be 0.4 eV, which suggested the intrinsic semiconducting nature of this charge-transfer complex (Figure S4B).

The DPTTA–DTTCNQ complex crystallized in a triclinic unit cell of P-1 space group with the unit cell parameters $a = 10.0529(18)$ Å, $b = 10.192(2)$ Å, $c = 10.312(2)$ Å, $\alpha = 86.863(9)°$, $\beta = 74.581(7)°$, $\gamma = 76.051(8)°$. In the crystal, the donor and acceptor molecules possess a symmetric center located at the center of the annulene and quinoid rings, respectively (**Figure 1**A). In DTTCNQ the thiophene units are disordered with the sulfur atoms appearing in the 1, 2, 4, 5-positions of the quinoid ring with 50 % occupancy, just as is observed in its individual crystal and complex with TTF.[21] In the DPTTA molecule, the center annulene moiety adopts a nearly coplanar structure with S(1), S(2), S(1A), and S(2A) atoms derived from the mean plane of 0.014, 0.105, −0.014, and −0.105 Å. Two phenyl groups keep the same dihedral angle (72.49°) as the main plane and are uniformly oriented; the angle is obviously smaller than that in the crystal of pure DPTTA (80.65°). For DTTCNQ in the co-crystal, the bond length of cyano groups (1.141(4), 1.139(4) Å) is slightly longer than that observed in the pristine DTTCNQ molecule (1.129, 1.135 Å),[21a] which indicates weak charge-transfer interactions between DPTTA and DTTCNQ. The DPTTA–DTTCNQ co-crystal has 1:1 stoichiometry, where the donor and acceptor molecules stack alternatively

into columns along the *c* axis (Figure 1B and 1C). A dihedral angle of 2.7° was observed between the molecular plane of DPTTA and DTTCNQ. The intermolecular distance between DPTTA and DTTCNQ is around 3.34 Å, which is obviously less than that of the typical distance of van der Waals interaction. In the stacking direction S···S short contacts (3.651 Å) between DPTTA (S(2)) and DTTCNQ (S(3A)) molecules could be observed. N···H–C and S···H–C hydrogen bonds could be observed between donor and acceptor molecules in adjacent columns (Figure 1B, 1C, and S5). Besides these intermolecular interactions between donor and acceptor molecules, direct π–π interactions among donor molecules in the neighboring columns also existed (Figure S6), as the shortest carbon–carbon distance is 3.321Å, which is shorter than twice the van der Waals radius of carbon (3.40 Å). For acceptor molecules, although the shortest nitrogen–nitrogen distance (3.290 Å) is slightly larger than the sum of two van der Waals radii of nitrogen atoms (3.10 Å), the interplane distance between these two molecules is only 3.02 Å, which indicates the existence of π–π interactions (Figure S6). So, continuous direction π–π interactions among donor molecules and acceptor molecules are expected to serve as a charge-transport path for holes and electrons respectively, as will be discussed in detail in the following section on quantum calculation. The overlap pattern of DPTTA–DTTCNQ complex in the crystal is illustrated in Figure 1D; despite the extended π-conjugated system of DTTCNQ, it overlaps with only half of the DTTCNQ molecule,
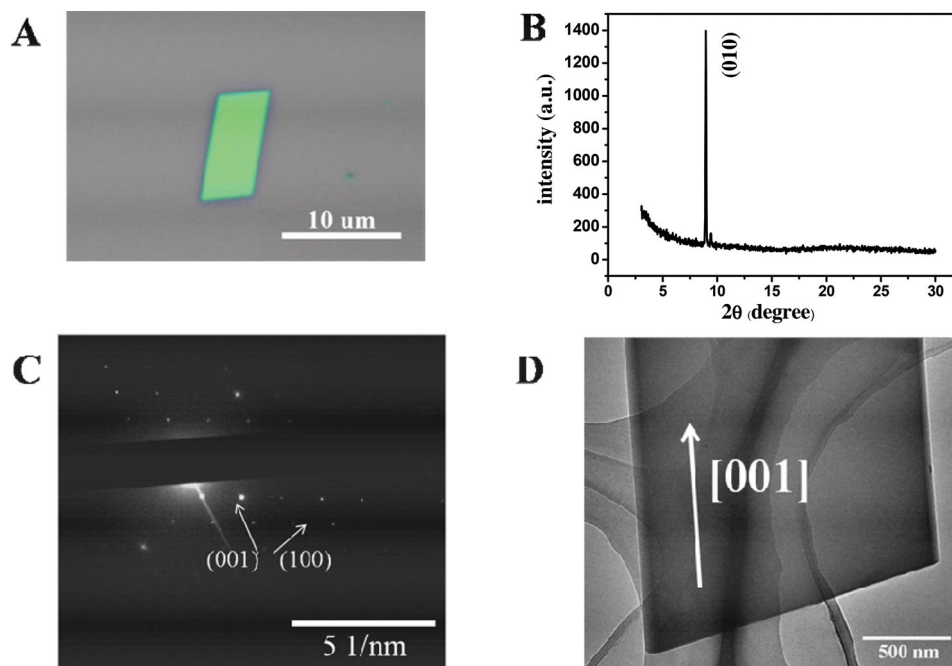
Figure 2. A) Optical image of individual DPTTA–DTTCNQ co-crystal nanosheet obtained by drop-casting. B) Powder diffraction pattern of the co-crystals. The peaks were indexed with lattice constants of the bulk crystals. C,D) SAED patterns of a crystalline nanosheet and its corresponding TEM image.

as observed in the DTPPA–TCNQ co-crystal. Considering the closer D–A distance and partial charge-transfer character in DPTTA–DTTCNQ than in DPTTA–TCNQ, stronger D–A interactions are expected than those previously reported, which may benefit the superexchange effect and enhance the electronic couplings along the stacking direction. This effect will be quantitatively analyzed in the following. Crystallographic data of the co-crystal are summarized in Table S1.

To characterize the transport properties of this crystal, we employed a simple drop-casting method to grow microcrystals of DPTTA–DTTCNQ on SiO_2/Si substrate. The microcrystals were obtained with high quality and suitable for device fabrication. As shown in **Figure 2**A, a parallelogram-shaped crystalline nanosheet with length of several micrometers and thickness of tens of nanometers was obtained after evaporating several drops of chlorobenzene solution containing equimolar amounts of DPTTA and DTTCNQ on SiO_2/Si substrate (for details, see the Experimental Section). The powder X-ray diffraction patterns (Figure 2B) of the nanosheets show an intense peak at 8.96°, which corresponds to a d spacing of 9.89 Å. This result can be well indexed to the (010) plane with the crystallographic data of the DPTTA–DTTCNQ crystal. To further investigate the packing orientation of the D–A complex, we conducted selected-area electron diffraction (SAED) with transmission electron microscopy (TEM) on a microcrystal grown on an amorphous carbon-coated TEM grid (Figure 2C,D). A single-crystal-like diffractive pattern was obtained in the SAED characterization. The in-plane lattice distances were calculated as 1.032 nm from the diffractive points. The distance coincides with the interplane distance of the (001) plane. By comparing the TEM image of the selected area, the preferential growth direction in the co-crystal is determined to be [001] (c axis) with the ac plane parallel to the substrate surface.

Au electrodes as source/drain electrodes were thermally evaporated on to the microcrystal to construct transistors with bottom-gate and top-contact geometry. **Figure 3**A,B shows a schematic diagram of this bottom-gate top-contact miniature transistor and an optical microscopy image of the device based on a single DPTTA–DTTCNQ nanosheet. More than 30 devices were measured and typical ambipolar properties were obtained under ambient conditions. The typical transfer and output characteristics of the device based on an individual crystalline nanosheet are shown in Figure 3C,D. Both the output and transfer characteristics demonstrate typical ambipolar transport behavior. The electron and hole field-effect mobilities (μ) were calculated as 0.24 cm^2 V^{-1} s^{-1} (μ_e) and 0.77 cm^2 V^{-1} s^{-1} (μ_h). The I_{on}/I_{off} ratio was 1.5×10^3 and 5×10^2, respectively. The histograms of mobility distribution from 32 devices based on D–A co-crystals are shown in Figure S7A. For hole transport, the hole mobility ranged from 0.13–0.81 cm^2 V^{-1} s^{-1}. For electron transport, the electron mobility ranged from 0.01–0.29 cm^2 V^{-1} s^{-1}. Moreover, the device exhibits good stability in air even after 180 days of storage in air. A typical evolution of performance versus storage time is shown in Figure S7B,C.

Compared to the highest mobility of DPTTA obtained in single-crystal transistors (0.7 cm^2 V^{-1} s^{-1}),[22] this DPTTA–DTTCNQ crystal has almost equivalent hole mobility. For electron transport, the mobility is improved by nearly an order of magnitude compared to that of pristine DTTCNQ thin films (Figure S8). The ambipolar transport performance of the DPTTA–DTTCNQ crystal is obviously higher than those of previously reported donor–acceptor complexes.
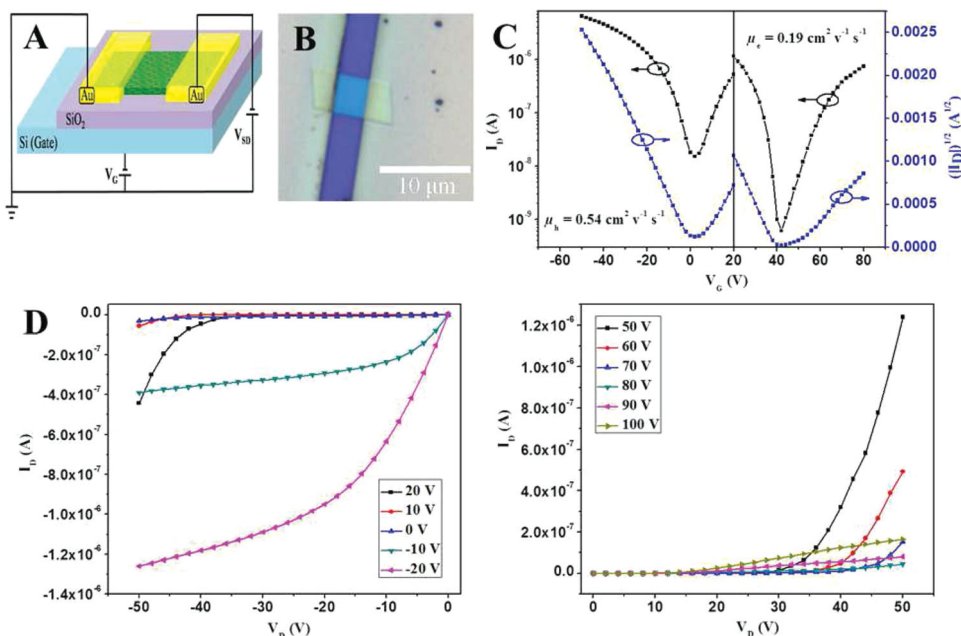
Figure 3. A) Schematic diagram of device structure. B) Optical image of the device with an individual nanosheet. C) Transfer and D) output characteristics (channel length, $L = 3.4 \ \mu m$, channel width, $W = 4.4 \ \mu m$) of the device.

Recent theoretical and experimental research on the mechanisms of electrical doping in organic semiconductors[23] and ambipolar transport behaviors of crystals of donor–acceptor complexes[9] revealed that formation of charge-transfer complexes could be an alternative strategy for the development of organic semiconductors, besides the chemical tailoring approach. The bandgap and bandwidth of the resulting complexes can be easily tuned by choosing appropriate donor or acceptor components, as the bandgap will be determined by the hybridization of the highest occupied molecular orbital (HOMO) of the donor molecule and lowest unoccupied molecular orbital (LUMO) of the acceptor molecules, while the electronic couplings for holes and electrons are a more complex issue related to D–A interaction strength, charge-transfer ratio, intermolecular relative orientation, and so on. As Zhu et al. pointed out,[9] the electronic coupling in a D–A complex is contributed both from direct interactions and superexchange interactions, and the latter could lead to electronic coupling as large as or even larger than that of the best single-component organic semiconductors. Here, DTTCNQ was employed with the initial aim of enhancing the superexchange interactions through the extension of the π-conjugated system of the acceptor molecule to match better with the donor molecule. To figure out the real mechanism for its superior performance, a detailed quantum calculation on its electronic couplings as well as reorganization energies of holes and electrons was carried out. Here, we present some preliminary calculation results.

Based on the B3LYP functional and 6–31G (d) basis sets implemented in Gaussian09,[24] the reorganization energy of electron and hole are 372 and 232 meV, respectively. Intermolecular electronic couplings were evaluated according to the crystal structure. Both direct D–D (A–A) electronic coupling through space (t_{direct}) and bridge-mediated electron coupling

with superexchange character (t_{super}) exist in this case, the main charge-transport path way as illustrated in **Figure 4**. The direct electronic coupling (t_{direct}) between the closest donor (acceptor) molecules along the a axis was calculated with the site-energy correction method,[25] and superexchange electronic coupling of hole and electron was calculated through energy splitting of D–A–D and A–D–A clusters, respectively.[9,10] The results indicate that there are moderate electronic couplings along the c axis due to the superexchange effects; the t_{super} values for electrons and holes are 53.6 and 23.4 meV, respectively. The t_{direct} values of electrons and holes are 26.4 and 41.4 meV, which are comparable or even larger than t_{super}. The DPTTA–DTTCNQ co-crystal possesses a quasi-2D ambipolar transport network in the ac plane. This result is obviously different from what we observed previously in DPTTA–TCNQ and DPTTA–fullerene crystals, where superexchange interactions dominate the electronic couplings in the former and only direct coupling exist in the latter complex. DPTTA–TCNQ displays a 1D conducting path along the stacking direction with almost equal t_{super} values of 62 and 63 meV for electrons and holes, which are larger than those in DPTTA–DTTCNQ crystals. Combined with a relatively larger reorganization energy of DTTCNQ compared to TCNQ (256 meV), inferior transport properties, especially for electrons, are expected for the DPTTA–DTTCNQ crystal. However, this conflicts with the experimental results. One possible interpretation is that, in a 1D crystal, the electrical transport should be more easily interrupted by the defects, whereas a crystal with 2D electrical transport network should possess higher tolerance towards the defects. We have previously observed a similar situation in single crystals of 6H-pyrrolo[3,2-b:4,5-b'] bis[1,4]benzothiazine and its derivatives.[26]

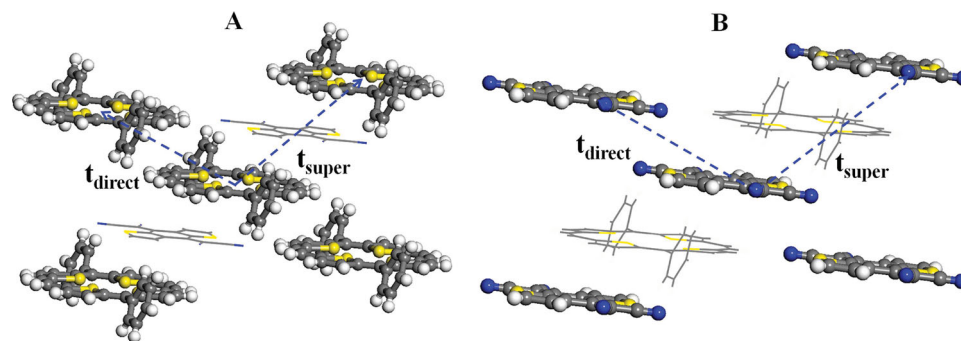We have successfully obtained a DPTTA-based charge-transfer complex with DTTCNQ and investigated its

Figure 4. The most important charge transport pathways and electronic coupling for hole and electron. A) Hole: t_{direct} = 41.4 meV, t_{super} = 23.4 meV. B) Electron: t_{direct} = 26.4 meV, t_{super} = 53.6 meV. t_{direct}, the direct electron coupling between the closest donor (acceptor) molecules along a axis; t_{super}, the effective electron coupling by a superexchange mechanism through the bridge molecule (donor molecule for electron transport, acceptor molecule for hole transport) along the c axis.

charge-transport properties. Single-crystal field-effect transistors based on this charge-transfer complex exhibits remarkably ambipolar behavior with a high hole mobility of 0.77 cm V^{-1} s^{-1} and electron mobility of 0.24 cm^2 V^{-1} s^{-1} in ambient atmosphere. Crystallographic analysis show that extension of the π-conjugated system of acceptor molecules and partial charge-transfer between donor and acceptor molecules enhanced the interactions between donors and acceptors and resulted in the formation of a quasi-2D ambipolar transport network. Quantum calculation on intermolecular electronic coupling gave further evidence on the 2D character of this crystal as both superexchange effect and direct coupling existed. This result offers a new way to improve the electrical transport properties of such D–A complex systems. Higher performance could be expected by further tuning the π-extension degree and electron affinity of the acceptor. The complex also provides a new ideal vehicle for further theoretical investigation of the relationship between packing structure, charge transfer, and performance.

Experimental Section

Materials: DPTTA was purchased from BioDuro. The product was further purified by recrystallization (in toluene and dichloromethane). DTTCNQ was synthesized by TiCl$_4$-mediated condensation of the corresponding quinone and malononitrile.[27] Under an argon atmosphere, pyridine (10 mL) was added to a magnetically stirred solution of the quinine (0.635 g, 2.88 mmol) and malononitrile (3.80 g, 57.5 mmol) in chloroform (200 mL). Then TiCl$_4$ (0.8 mL, 5.8 mmol) was slowly injected into the reaction solution through a syringe. The reaction mixture was refluxed for 5 h and then cooled to room temperature. Water (400 mL) was added and then the insoluble solid filtered off. The organic layer was collected and dried with anhydrous MgSO$_4$. After removing the organic solvent by rotary evaporation, the crude product was purified by silica gel chromatography with chloroform as eluent to afford the desired red product.

Single crystals of DPTTA–DTTCNQ suitable for X-ray analysis, IR, DRS, and ESR were obtained as shiny black flakes with elongated parallelogram shapes by slow evaporation of the chlorobenzene solution (molar ratio 1:1) after heating at 120 °C for several minutes.

Growth of the Self-Assembled Microcrystal and Device Fabrication: The SiO$_2$/Si substrate was a heavily doped n-type Si wafer with a 500-nm-thick SiO$_2$ layer and a capacitance of 7.5 nF cm^{-2}. Bare substrates were successively cleaned with pure water, hot concentrated sulfuric acid–hydrogen peroxide solution (H$_2$SO$_4$:H$_2$O$_2$ = 2:1), pure water, and pure

isopropanol. The self-assembled co-crystal was conducted by using the drop-casting method. In a typical preparation progress, 0.5–1 mg mL^{-1} solution in chlorobenzene (DPTTA and DTTCNQ with a molar ratio of 1:1) was poured over the substrates and the solvent evaporated at room temperature. Drain and source Au electrodes (50-nm thick) were deposited on the microcrystal by thermal evaporation using the organic-ribbon mask method.[28]

Measurements: UV-vis spectra were taken on a Hitachi U-3010 spectrometer. IR spectra were recorded on a TENSOR 27 instrument (BRUKER, GERMANY). ESR experiments were conducted on a Bruker EPR ELEXSYS 500 spectrometer (Bruker Co. Germany) with a resonance frequency of 9.77 GHz. The DRS was obtained from Shimadzu UV-3600. TEM and SAED measurements were carried out on a JEOL 2010 (Japan). X-ray diffraction (XRD) was measured on D/max2500 with CuKa source (κ = 1.541 Å). I–V characteristics of the OFETs were recorded with a Keithley 4200 SCS and a Micromanipulator 6150 probe station in a clean and shielded box at room temperature in air. The mobilities (μ) were calculated in the saturation regime by using the following equation: $I_D = \mu C_i (W/2L)(V_G - V_T)^2$, where I_D is the drain current, μ is the field-effect mobility, C_i is the gate dielectric capacitance, W and L are the channel width and length, respectively, and V_T is the threshold voltage.

X-ray crystallographic data were collected with a Bruker Smart-1000-CCD diffractometer, using graphite-monochromated Mo Kα radiation (λ = 0.71073 Å). The data were collected at 113 K and the structure was resolved by the direct method and refined by the full-matrix least-squares method on F^2. The computations were performed with the SHELXL-97 program.[29] The final refinement was anisotropic for all non-H atoms.

Supporting Information

Supporting Information is available from the Wiley Online Library or from the author.

Acknowledgements

[1] a) Z. G. Soos, *Annu. Rev. Phys. Chem.* **1974**, *25*, 121; b) S. Horiuchi, T. Hasegawa, Y. Tokura, *J. Phys. Soc. Jpn.* **2006**, *75*, 051016; c) T. Mori, *Chem. Lett.* **2011**, *40*, 428.

[2] a) P. Batail, *Chem. Rev.* **2004**, *104*, 4887; b) J. Ferraris, D. O. Cowan, J. V. Walatka, J. H. Perlstein, *J. Am. Chem. Soc.* **1973**, *95*, 948; c) A. Girlando, A. Painelli, C. Pecile, G. Calestani, C. Rizzoli, R. M. Metzger, *J. Chem. Phys.* **1993**, *98*, 7692; d) K. V. Rao, S. J. George, *Chem. Eur. J.* **2012**, *18*, 14286.

[3] a) A. S. Tayi, A. K. Shveyd, A. C. Sue, J. M. Szarko, B. S. Rolczynski, D. Cao, T. J. Kennedy, A. A. Sarjeant, C. L. Stern, W. F. Paxton, W. Wu, S. K. Dey, A. C. Fahrenbach, J. R. Guest, H. Mohseni, L. X. Chen, K. L. Wang, J. F. Stoddart, S. I. Stupp, *Nature* **2012**, *488*, 485; b) S. Horiuchi, Y. Tokura, *Nat. Mater.* **2008**, *7*, 357; c) G. Giovannetti, S. Kumar, A. Stroppa, J. van den Brink, S. Picozzi, *Phys. Rev. Lett.* **2009**, 103.

[4] a) S. J. Kang, J. B. Kim, C. Y. Chiu, S. Ahn, T. Schiros, S. S. Lee, K. G. Yager, M. F. Toney, Y. L. Loo, C. Nuckolls, *Angew. Chem. Int. Ed.* **2012**, *51*, 8594; b) S. J. Kang, S. Ahn, J. B. Kim, C. Schenck, A. M. Hiszpanski, S. Oh, T. Schiros, Y. L. Loo, C. Nuckolls, *J. Am. Chem. Soc.* **2013**, *135*, 2207.

[5] a) D. Yan, A. Delori, G. O. Lloyd, T. Friscic, G. M. Day, W. Jones, J. Lu, M. Wei, D. G. Evans, X. Duan, *Angew. Chem. Int. Ed.* **2011**, *50*, 12483; b) T. Wakahara, M. Sathish, K. i. Miyazawa, C. Hu, Y. Tateyama, Y. Nemoto, T. Sasaki, O. Ito, *J. Am. Chem. Soc.* **2009**, *131*, 9940; c) Y. L. Lei, Y. Jin, D. Y. Zhou, W. Gu, X. B. Shi, L. S. Liao, S. T. Lee, *Adv. Mater.* **2012**, *24*, 5345; d) K. R. Leight, B. E. Esarey, A. E. Murray, J. J. Reczek, *Chem. Mater.* **2012**, *24*, 3318.

[6] T. Hasegawa, K. Mattenberger, J. Takeya, B. Batlogg, *Phys. Rev. B* **2004**, *69*, 245115.

[7] Y. Takahashi, T. Hasegawa, Y. Abe, Y. Tokura, G. Saito, *Appl. Phys. Lett.* **2006**, *88*, 073504.

[8] M. Sakai, H. Sakuma, Y. Ito, A. Saito, M. Nakamura, K. Kudo, *Phys. Rev. B* **2007**, *76*, 045111.

[9] L. Zhu, Y. Yi, Y. Li, E. G. Kim, V. Coropceanu, J. L. Bredas, *J. Am. Chem. Soc.* **2012**, *134*, 2340.

[10] J. Zhang, H. Geng, T. S. Virk, Y. Zhao, J. Tan, C. A. Di, W. Xu, K. Singh, W. Hu, Z. Shuai, Y. Liu, D. Zhu, *Adv. Mater.* **2012**, *24*, 2603.

[11] J. Zhang, J. Tan, Z. Ma, W. Xu, G. Zhao, H. Geng, C. Di, W. Hu, Z. Shuai, K. Singh, D. Zhu, *J. Am. Chem. Soc.* **2013**, *135*, 558.

[12] T. Wakahara, P. D'Angelo, K. Miyazawa, Y. Nemoto, O. Ito, N. Tanigaki, D. D. C. Bradley, T. D. Anthopoulos, *J. Am. Chem. Soc.* **2012**, *134*, 7204.

[13] S. K. Park, S. Varghese, J. H. Kim, S. J. Yoon, O. K. Kwon, B. K. An, J. Gierschner, S. Y. Park, *J. Am. Chem. Soc.* **2013**, *135*, 4757.

[14] H.-D. Wu, F.-X. Wang, Y. Xiao, G.-B. Pan, *J. Mater. Chem. C* **2013**, *1*, 2286.

[15] K. Singh, A. Sharma, J. Zhang, W. Xu, D. Zhu, *Chem. Commun.* **2011**, *47*, 905.

[16] a) K. Kobayashi, C. L. Gajurel, *J. Chem. Soc., Chem. Commun.* **1986**, 1779; b) K. Kobayashi, C. T. Pedersen, J. Becher, *Phosphorus, Sulfur Silicon Relat. Elem.* **1989**, *43*, 187; c) M. Yasui, M. Hirota, Y. Endo, F. Iwasakii, K. Kobayashi, *Bull. Chem. Soc. Jpn.* **1992**, *65*, 2187.

[17] a) D. M. de Leeuw, M. M. J. Simenon, A. R. Brown, R. E. F. Einerhand, *Synth. Met.* **1997**, *87*, 53; b) C. M. Cardona, W. Li, A. E. Kaifer, D. Stockdale, G. C. Bazan, *Adv. Mater.* **2011**, *23*, 2367.

[18] a) J. S. Chappell, A. N. Bloch, W. A. Bryden, M. Maxfield, T. O. Poehler, D. O. Cowan, *J. Am. Chem. Soc.* **1981**, *103*, 2442; b) S. Caillieux, D. de Caro, L. Valade, M. Basso-Bert, C. Faulmann, I. Malfant, H. Casellas, L. Ouahab, J. Fraxedas, A. Zwick, *J. Mater. Chem.* **2003**, *13*, 2931; c) X. Chi, C. Besnard, V. K. Thorsmølle, V. Y. Butko, A. J. Taylor, T. Siegrist, A. P. Ramirez, *Chem. Mater.* **2004**, *16*, 5751.

[19] P. L. Maguères, S. V. Lindeman, J. K. Kochi, *J. Chem. Soc., Perkin Trans. 2*, **2001**, 1180.

[20] a) C. He, M. Gu, *Scri. Mater.* **2006**, *55*, 481; b) B. Zhou, J. Qu, X. Zhao, H. Liu, *J. Environ. Sci.* **2011**, *23*, 151.

[21] a) F. Iwasaki, N. Toyoda, M. Hirota, N. Yamazaki, M. Yasui, K. Kobayashi, *Bull. Chem. Soc. Jpn.* **1992**, *65*, 2173; b) F. Iwasaki, S. Hironaka, N. Yamazaki, K. Kobayashi, *Bull. Chem. Soc. Jpn.* **1992**, *65*, 2180.

[22] J. Zhang, Z. Ma, Q. Zhang, T. S. Virk, H. Geng, D. Wang, W. Xu, Z. Shuai, K. Singh, W. Hu, D. Zhu, *J. Mater. Chem. C* **2013**, *1*, 5765.

[23] a) I. Salzmann, G. Heimel, S. Duhm, M. Oehzelt, P. Pingel, B. M. George, A. Schnegg, K. Lips, R.-P. Blum, A. Vollmer, N. Koch, *Phys. Rev. Lett.* **2012**, *108*, 035502; b) H. Mendez, G. Heimel, A. Opitz, K. Sauer, P. Barkowski, M. Oehzelt, J. Soeda, T. Okamoto, J. Takeya, J. B. Arlin, J. Y. Balandier, Y. Geerts, N. Koch, I. Salzmann, *Angew. Chem. Int. Ed.* **2013**, *52*, 7751.

[24] M. J. Frisch, G. W. Trucks, H. B. Schlegel, G. E. Scuseria, M. A. Robb, J. R. Cheeseman, G. Scalmani, V. Barone, B. Mennucci, G. A. Petersson, H. Nakatsuji, M. Caricato, X. Li, H. P. Hratchian, A. F. Izmaylov, J. Bloino, G. Zheng, J. L. Sonnenberg, M. Hada, M. Ehara, K. Toyota, R. Fukuda, J. Hasegawa, M. Ishida, T. Nakajima, Y. Honda, O. Kitao, H. Nakai, T. Vreven, J. A. Montgomery, J. E. Peralta, F. Ogliaro, M. Bearpark, E. B. J. J. Heyd, K. N. Kudin, V. N. Staroverov, R. Kobayashi, J. Normand, K. Raghavachari, A. Rendell, J. C. Burant, S. S. Iyengar, J. Tomasi, M. Cossi, N. Rega, J. M. Millam, M. Klene, J. E. Knox, J. B. Cross, V. Bakken, C. Adamo, J. Jaramillo, R. Gomperts, R. E. Stratmann, A. O. Yazyev, J. Austin, R. Cammi, C. Pomelli, J. W. Ochterski, R. L. Martin, K. Morokuma, V. G. Zakrzewski, G. A. Voth, P. Salvador, J. J. Dannenberg, A. S. Dapprich, D. Daniels, O. Farkas, J. B. Foresman, J. V. Ortiz, J. Cioslowski, D. J. Fox, *Gaussian 09, Revision A.02, Gaussian, Inc., Wallingford CT*, **2009**.

[25] E. F. Valeev, V. Coropceanu, D. A. d. S. Filho, S. Salman, J.-L. Bredas, *J. Am. Chem. Soc.* **2006**, *128*, 9882.

[26] Z. Wei, W. Hong, H. Geng, C. Wang, Y. Liu, R. Li, W. Xu, Z. Shuai, W. Hu, Q. Wang, D. Zhu, *Adv. Mater.* **2010**, *22*, 2458.

[27] K. Kobayashi, C. L. Gajurel, K. Umemoto, Y. Mazaki, *Bull. Chem. Soc. Jpn.* **1992**, *65*, 2168

[28] L. Jiang, J. Gao, E. Wang, H. Li, Z. Wang, W. Hu, L. Jiang, *Adv. Mater.* **2008**, *20*, 2735.

[29] G. M. Sheldrick, SHELXL97, *Program for the Refinement of Crystal Structure* **1997**, University of Göttingen, Germany.